Reactive amine surfaces for biosensor applications, prepared by plasma-enhanced chemical vapour modification of polyolefin materials

C. Volcke[1, 2, *, §], R.P. Gandhiraman[1, *], V. Gubala[1], J. Raj[3], Th. Cummins[1, 4], G. Fonder[5], R.I. Nooney[1], Z. Mekhalif[5], G. Herzog[3], S. Daniels[1, 6], D.W.M. Arrigan[3,#], A.A. Cafolla[1, 4] and D.E. Williams[1, 7]

[1] *Biomedical Diagnostics Institute, Dublin City University, Glasnevin, Dublin 9, Ireland.*

[2] *Research Centre in Physics of Matter and Radiation, University of Namur (FUNDP), 61 rue de Bruxelles, 5000 Namur, Belgium.*

[3] *Biomedical Diagnostics Institute Programme, Tyndall National Institute, University College Cork, Cork, Ireland.*

[4] *School of Physical Sciences, Dublin City University, Glasnevin, Dublin 9, Ireland.*

[5] *Laboratory of Chemistry and Electrochemistry of Surfaces, University of Namur (FUNDP), 61 rue de Bruxelles, 5000 Namur, Belgium.*

[6] *National Center for Plasma Science and Technology, Dublin City University, Glasnevin, Dublin 9, Ireland.*

[7] *MacDiarmid Institute for Advanced Materials and Nanotechnology, Department of Chemistry, University of Auckland, Private Bag 92019, Auckland 1142, New Zealand.*

Abstract

Here we have demonstrated a solventless plasma-based process that integrates low-cost, high throughput, high reproducibility and ecofriendly process for the functionalization of the next-generation point-of-care device platforms. Amine functionalities were deposited by plasma-enhanced chemical vapour deposition (PECVD) using a new precursor. The influence of the plasma RF power and the deposition time on surfacial properties, as well as their effect on the reactivity and content of amino groups was investigated. The key process determinants were to have a sufficient power in the plasma to activate and partially fragment the monomer but not too much as to lose the reactive amine functionality, and sufficient deposition time to develop a reactive layer but not to consume or erode the amine reactivity. An immunoassay performed using human immunoglobulin (IgG) as a model analyte showed an improvement of

the detection limit by two orders of magnitude beyond that obtained using devices activated by liquid-phase reaction.

Keywords: biosensors, polymer, plasma enhanced chemical vapour deposition, nanoparticle, DNA, immunoassay.

* Those authors contributed equally

§ Corresponding author. Phone: +32 81 72 54 30. Fax: +32 81 72 47 18. E-mail : cedric.volcke@fundp.ac.be

Current address: Nanochemistry Research Institute, Department of Chemistry, Curtin University of Technology, GPO Box U1987, Perth, WA 6845, Australia.

1. Introduction

Immobilization of biomolecules onto surfaces, and particularly onto polymeric substrates, is a key issue for the fabrication of next-generation biosensor devices. In this context, a new class of polymeric materials, cyclo olefin polymers (COP), has received particular attention. Zeonor® is one such COP polymer presenting excellent optical properties, good chemical resistance, ease of fabrication and cost effectiveness (Diaz-Quijada 2007). These properties make Zeonor® particularly well-suited for sophisticated microchip designs including optical detection in biomedical and molecular diagnostic sensors.

Though several biomolecule immobilization techniques are reported in the literature, only a few recent communications address the issue of COP activation (Jönsson 2008, Raj 2009). In general, biomolecule immobilization is classified as chemical (Mateo-Marti 2005) or physical (LaGraff and Chu-LaGraff 2006). Chemical immobilization, through covalent linkage of biomolecules onto surfaces has shown good reproducibility and coverage, therefore becoming predominant. In such cases, liquid-phase deposition of functional groups, further attaching biomolecules, on activated surfaces is a routinely used procedure. For example, self-assembly of aminosilanes on oxidized silicon is one of the most studied methods (Song 2008, Zhang and Srinivasan 2004). These modification procedures are still not extensively investigated for polymers, for which physical immobilization is the dominant methodology.

Liquid-phase deposition of aminosilanes onto surfaces is demanding (water-free environment, time-consuming, hazardous materials) and hardly applicable to large industrial production requirements (Kurth and Bein 1995). Oppositely, gas-phase deposition of amine reactive groups, using plasma-enhanced chemical vapour deposition (PECVD) for example, overcomes the drawbacks of liquid-phase deposition (White and Tripp 2000). PECVD has proven to be an excellent tool for surface modification at low temperatures (Dudek 2009a, Gandhiraman 2007, Muguruma and Kase 2006). In principle, it offers significant advantages:

uniformly diverse functional coating deposition on various surfaces; precise control of thickness; and adaptability for large mass production processing. Moreover, surface amination by PECVD was previously studied using, e.g., ethylene diamine (EDA) as precursor (Jung 2006). Unfortunately, the adhesion and stability of these EDA films onto COP were very poor (unpublished data). The results were interpreted to imply merely physisorption and not reactive chemisorption of EDA molecules onto the polymeric surface.

New precursors, potentially presenting good adhesion and stability on polymeric surfaces, and also offering amine groups for subsequent reaction, are therefore needed. In this context, 3-(aminopropyl)triethoxysilane (APTES), commonly used for liquid-phase deposition (Qian 1999, Simon 2002) is expected to present all the requirements needed, expecting to result in reproducible silanized surfaces containing reactive amine groups, with good adhesion to COP through a siloxane network. COP substrates so functionalized could allow covalent attachment of highly dense antibodies and DNA molecules, used as target molecules in biosensor devices, therefore increasing limit of detection of the designed biosensor devices. The versatility, reproducibility and stability of this technique is expected to be applicable to a wide range of polymeric substrates for easy and rapid enhancement of actual (like ELISA) and future biosensors application properties through, amongst other, higher attachment of target proteins.

In this paper, we present a detailed investigation on the optimization of the reactive-amine content of a deposited amino-film on a COP surface, for improved biomolecule attachment by appropriate choice of experimental parameters. Aminated coatings were prepared by PECVD of APTES onto a Zeonor® substrate. The influence of the plasma RF power and the deposition time on the deposited amount of amino functionalities and on their capacity for immobilizing nano-size objects (nanoparticles) and biomolecules (ssDNA) was

investigated. Water contact angles (WCA), atomic force microscopy (AFM), ellipsometry and polarization modulation infrared reflection-absorption spectroscopy (PMIRRAS) were used for physical and chemical characterization. Fluorescence microscopy was performed to quantify the binding capacity of nanoparticles, amine-reactive fluorophore and labelled ssDNA molecules. An immunoassay was performed using human immunoglobulin G (IgG) as a model analyte.

2. Experimental Part

2.1. Materials

Plain Zeonor® slides (1060R) were obtained from Åmic AB (Uppsala, Sweden). 3-aminopropyltriethoxysilane (APTES), Lissamine® rhodamine B sulfonyl chloride ($\lambda_{exc.}$ = 532 nm excitation and λ_{em} = 550 nm emission, further denominated as lissamine), acetonitrile, high purity HPLC grade water, glutaraldehyde, triethylamine, sodium dodecyl sulphate (SDS), pyridine, Tween 20®, dimethylformamide (DMF), 2-(N-morpholino)ethanesulfonic acid (MES) buffer, $MgCl_2$, methanol, phosphate buffered saline (PBS) solution, bovine serum albumin (BSA), the model analyte human IgG (IgG), capture antibody goat anti-human IgG (gαIgG) and Cy-5 labelled gαIgG were obtained from Sigma-Aldrich. ssDNA were obtained from MWG Biotech. 1-ethyl-3(3-dimethylaminopropyl)carbodiimide and N-hydroxysulfosuccinimide were purchased by Pierce. ABCR provided 1,4-phenyldithioisocyanate (PDITC).

2.2. PECVD system

The plasma deposition was carried out using a computer controlled Europlasma CD 300 PECVD system. The vacuum chamber was connected to a Dressler's CESAR 136 RF power source operating at 13.56 MHz, supplied with an automated impedance match-box for effective RF energy input to the plasma. The detailed description and a schematic of the system used is shown elsewhere (Dudek 2009b, Gandhiraman 2009).

2.3. Surface preparation

Dry air cleaned Zeonor® slides were introduced into the chamber before pumping down to a base pressure of 25 mTorr. APTES precursor stored in a heated container was connected to the chamber through a heated supply line (both at 80° C). Plasma pre-treatment was carried out using a mix of argon (50 sccm) and oxygen (50 sccm) plasma at 250 watt RF power for 3 minutes. The oxygen supply was then closed and the plasma RF power decreased to the

desired value. APTES was then introduced in the chamber for the required deposition time. The operating pressure was ~ 70 mTorr.

2.4. Surface characterization

2.4.1. Ellipsometry

The thickness of the APTES coatings on Zeonor® was characterized using J.A. Woollam Co., Inc EC-400, M-2000UI Spectroscopic Ellipsometer. All layers were modelled as a simple silicon dioxide dispersion layer to extract an effective thickness.

2.4.2. WCA

The film wettability was analyzed by measuring the water contact angle of the film surface (First Ten Angstroms FTA200 contact angle analyser). High purity HPLC grade water was used.

2.4.3. Roughness measurements

AFM examinations were performed in ambient air with a commercial microscope (Dimension 3100 controlled by a Nanoscope IIIa controller, Digital Instruments), in the Tapping-Mode™, using standard silicon cantilevers (BudgetSensors®) with a 7 nm radius of curvature and a 42 $N.m^{-1}$ spring constant (nominal values). Topography was recorded at a scanning rate of 1-2 Hz, and a resonance frequency of about 300 kHz (nominal value). The surface roughness was evaluated over 3 AFM images (5 µm x 5 µm, Supporting Informations) and the standard deviation was then calculated. The root-mean-square roughness was defined as the average of height deviations taken from the mean plane (Haidopoulos 2007).

2.4.4. PMIRRAS

Substrates for PMIRRAS measurements were prepared following a procedure described elsewhere (Jönsson 2008) and detailed in the Supporting Informations. PMIRRAS spectra were recorded on a Bruker Equinox 55-PMA37 spectra equipped with liquid nitrogen cooled mercury cadmium-telluride (MCT) detector and a zinc-selenide photoelastic modulator. The infrared light was modulated between s- and p-polarization at a frequency of 50 kHz. The incident angle upon the sample surface was around 85°. Signals generated from each polarization (Rs and Rp) were detected simultaneously by a lock-in amplifier and used to calculate the differential surface reflectivity ($\Delta R/R$) = (Rp - Rs)/(Rp + Rs). The spectra were an average of 640 scans and were taken at a spectral resolution of 2 cm^{-1}.

2.4.5. Nanoparticle (NP) approach

Amino-functionalized silica NPs were prepared using a microemulsion method described previously (Arriagada and Osseo-Asare 1999) and detailed in the Supporting Informations. The APTES coated COP slides were dipped in an aqueous solution containing glutaraldehyde (2 wt %) for 24 hrs. Following this the slides were immersed in the amino-coated NPs solution (2.0 mg / ml) for a further 24 hrs, before intensive rinsing with DI water. After this procedure, the NPs are covalently bound to coated COP surface. The NPs surface coverage was determined using AFM in conditions similar to roughness measurements. Nanoparticle counting was performed using the commercial Scanning Probe Image Processor program (SPIP™, version 4.1.8.0 from Image Metrology).

2.4.6. Fluorescence

Fluorophore attachment to aminated COP substrates was achieved by immersing the samples for 1 hr in a 0.23 mM lissamine in acetonitrile. 100 µl triethylamine was added to 100 ml of

the lissamine solution. Samples were then rinsed with distilled water and sonicated for 5 minutes in a 0.1 % SDS solution. Following, the substrates were rinsed again with distilled water and dried under a nitrogen stream. The fluorescence intensity was then measured using a plate scanner (GMS 418 scanner: Genetic Microsystems, Affymetrix). For the immobilization of fluorescently labelled DNA, slides were activated with PDITC linker by incubation of coated substrates for 3 hrs in a 5 mM solution of PDITC in anhydrous acetonitrile containing 1 wt % of pyridine. The slides were then washed three times in DMF and dried in a stream of nitrogen.

Afterwards, 50 10^{-7} M solution of the polynucleotide (5'-fluorescein labelled, 3'- C6 amino linker) was prepared by diluting the stock solution of ssDNA in 10 mM MES buffer containing 5 mM 1-ethyl-3(3-dimethylaminopropyl)carbodiimide, 10 mM $MgCl_2$ and 0.33 mM N-hydroxysulfosuccinimide. For post-processing, the slides were sonicated in 1% SDS for 5 minutes to remove the non-covalently bound ssDNA from the surface and then rinsed extensively with deionized water. The fluorescence intensity was then measured by the plate scanner.

2.5. Immunoassay

APTES modified slides were immersed in a 25 mM PDITC in DMF:pyridine (9:1 v/v) solution for two hours, before rinsing with DMF and methanol and drying under a stream of nitrogen. For the immunoassay, 1 µl of the capture antibody, gαIgG (0.1 mg/ml) solution, at the desired concentration, was loaded on a PDITC-modified slide and incubated at 37° C for one hour. The surfaces were then washed with PBS containing Tween 20 (0.2 % v/v) and further with PBS. The slides were subsequently immersed in a BSA (3 % w/v) solution for one hour. After rinsing with PBS, different concentrations of the model analyte IgG (0.02

pg/ml – 0.2 mg/ml) were loaded (1 μl) and incubated at 37° C for one hour. The slides were washed with PBS, then the detection antibody Cy-5 labelled gαIgG (1 μl of 0.3 mg/ml) was printed using BioRobotics pins (1 μl) and incubated at 37^{o} C for 1 hour. The device surfaces were subsequently washed with PBS containing Tween 20 (0.2 %) solution twice, with PBS once and dried under a stream of nitrogen. The immunoassay was then ready for detection by measuring the fluorescence intensity Fluorescence images were acquired with an Olympus BX51 Epi-fluorescent microscope equipped with an Olympus DP71 Camera and appropriate filters. The excitation was obtained using an X-Cite Lamp Series 120 PC.

3. Results and Discussion

PECVD deposited coatings were prepared under different conditions of RF plasma power at fixed deposition time (4 min), and of deposition time at fixed RF plasma power (14 watt). We first present results obtained on coating deposited at fixed deposition time and further at fixed RF plasma power, followed by the selection of the one in each batch having the highest amount of amino-groups. The surface reactivity was analyzed through nanoparticle, fluorophore and DNA attachment experiments. Finally immunoassay results are presented.

3.1. At fixed deposition time of 4 minutes

For coatings obtained at 7 watt, 14 watt and 25 watt RF power after 4 minutes deposition, the layer thickness, WCA and surface roughness values are presented in Table 1. Although variations highlighted in Table 1 are relatively small, the thickness clearly increased, at first steeply, and then more gradually, with increasing plasma RF power. These values are relevant with the formation of a thick layer, and not a monolayer. Although the species present into the plasma are not known into details, it could however be admitted that the coating formation can be explained as follows: the decomposition of the monomer (APTES) into fragment is induced by the plasma. These fragments are then depositing and covalently binding to the activated surface and to each other in order to form a fairly non-organized thick coating. Plasma electron density measurements using a hair pin probe (Supporting Informations) show that electron density (and hence plasma density) increased with increasing RF plasma power. The increased deposited thickness can therefore be explained as a consequence of the enhanced decomposition of the reactants induced by an increase in the plasma density, as previously reported for similar systems (Kulisch 1998).

Table 1

The equilibrium WCA highlight similar values for the three surfaces: around 55-60°. Thus, after coating deposition, the surface are more hydrophilic compared to plain COP (~ 92°), as expected. Moreover, the three coatings had similar hydrophilicity, independently of the plasma power used and is similar to literature values for liquid-phase deposited APTES molecules on silicon oxide surfaces (Cho and Ivanisevic 2004). All coatings were also very smooth (roughness values between 0.7 and 1.4 nm, Table 1). A uniform deposition over the polymeric surface, independently of the plasma power condition used, therefore occurred. It is noteworthy that roughness modifications due to uncontrolled aminosilane polymerization on the surface were not present here, illustrating one advantage of the PECVD deposition process.

The coatings PMIRRAS spectra (Figure 1) contain several vibrational features (missing on uncoated substrate spectrum) associated to bulk content of the deposited aminosilane coating, the most prominent being located in the 1300 - 1000 cm^{-1}, 1800 - 1500 cm^{-1} and 3500 - 3200 cm^{-1} regions (Figure 1; Region 1, 2 and 3 respectively).

Figure 1

Bands in Region 1 have three main components located at 1265 cm^{-1}, 1220 cm^{-1} and 1199 cm^{-1}. These are assigned to symmetric deformation of Si-CH_3 (1265 cm^{-1}), Si-CH_2-R deformation (1220 cm^{-1}), and Si-O-C and C-N vibrations (1199 cm^{-1}) (Socrates 2004, Wavhal 2006). Some variations in the IR absorption peak intensities are also observed. We can reasonably assume an isotropic orientation of the deposited molecules in the coating and an

independency of the orientation of the (fragmented) molecules with the deposition conditions used, so that IR peak intensities can be correlated to the amount of molecules/functional groups in the surface and the bulk of the coating, without taking into account orientation effects. The analysis of the peak intensities in Region 1 revealed peaks were generally more intense for the 7 watt coating, with a decreasing tendency in peak intensities as the RF plasma power increase. Thus, although the deposited layer thickness increased with increasing power, the silicon content of the layer decreased.

In Region 2 (Figure 1), the presence of carboxylic group vibrational peaks (at 1754 cm^{-1} and 1734 cm^{-1} associated to ν(C=O) ester and ν(C=O) carboxylic acid) was observed (Dreesen 2007) and their intensity varied following the trend:

$$I(C=O)_{25\ watt} < I(C=O)_{7\ watt} < I(C=O)_{14\ watt}$$

Oxygenated surface species could originate from the initial surface treatment but pretreatment conditions were identical for all coatings, which should not affect the C=O peak intensity. Therefore this trend is related to dissociation of the silane producing ethoxy radicals. The observed intensity variations arise from reactions of the carboxylic groups with radicals from APTES monomer molecules, as previously obtained under similar conditions using different monomers (Bae 2007). As the radicals created in the plasma differ according to plasma power conditions, they would react differently with the surface and a variable C=O vibration intensity is thus expected.

Vibrations associated with primary NH_2 vibrations are also identified in the 1650-1600 cm^{-1} range (Region 2, Figure 1). With increasing RF plasma power, this amine peak was slightly shifted towards lower wavenumbers, indicative of the transformation of free amines into hydrogen-bonded amines (Kanan 2002). A broad band associated to the presence of primary amines was also observed on all coatings in the range 3500-3200 cm^{-1} (Region 3, Figure 1). The NH_2 vibration intensity in both Region 2 and 3 were highest in the 7 watt

coating spectrum. The decrease in the NH_2 IR absorption bands with increase in the RF plasma power implies a decrease in the amine content of the coatings. The results indicate that, at the lowest power, the silane was activated and could react with the surface, but was not significantly dissociated. With increasing power, the silane became fragmented, with amine functions being lost and the layer being built through reaction of ethoxy radicals.

3.2. At fixed power

At fixed plasma power (14 watt), as the deposition time increased, the coating thickness also increased (Table 1). Again, the measured values are relevant with the formation of a non-organized thick multilayer. The WCA values (Table 1) showed that the hydrophilicity varied from ~ 92° for plain COP to ~ 60° after coating deposition, as expected. However, it was similar amongst the coatings considered. Moreover, all coatings were very smooth (roughness values between 0.7 and 1.3 nm, Table 1). Values were similar for all conditions, including plasma power variation, indicating the invariance of the roughness with the deposition condition.

Figure 2

Figure 2 highlights changes in the PMIRRAS spectra of the bulk and surface of the coating with varying deposition time. All peaks in the 1100 - 1300cm^{-1} region (Region 1, Figure 2) associated with silane vibration increased with increasing deposition time. The peak centred around 1200 - 1170 cm^{-1} (Si-O-C rocking and C-N vibrations) and around 1230 - 1210 cm^{-1} (Si-CH_2-R vibration) increased slightly in wavenumber with increasing deposition time (Socrates 2004). The peak intensities associated with amine and carboxylate functions, at

around 1700 cm^{-1} (Region 2, Figure 2) and 3200 - 3500 cm^{-1} (Region 3, Figure 2) followed the trend:

$$[NH_2, C=O]_{8\ min} < [NH_2, C=O]_{2\ min} < [NH_2, C=O]_{4\ min}$$

There were also changes in peak position in the amine region (Region 2, Figure 2). The 2 min, 4 min and 8 min coating presented a peak centred at 1594 cm^{-1}, at 1624 cm^{-1} and at 1644 cm^{-1}, respectively, indicative of an increase in the hydrogen-bonded character of the amino groups (Kanan 2002).

As deposition time increased, the thickness of the deposited layer increased. However, for deposition times longer than 4 min, the ester and amine amount decreased with increasing deposition time. We rationalize this by the fact that, during the plasma deposition, the growing film surface is exposed to the plasma. Therefore, as the plasma exposure time is increased, the reactive groups on the growing film surface, including amines and esters, might undergo functional changes induced by plasma generated species such as ions and charged radicals (Kim 2003). The maximum peak intensity assigned to amines was observed at deposition time of 4 min. This appeared to be the optimal condition at which a reasonable mass of amines could be formed on the surface. Longer exposure to the plasma seemed to trigger structural changes of the functional groups of interest.

3.3. Reactivity and binding capacity.

In the nanoparticle approach, a homo-bifunctional cross-linker, glutaraldehyde, was used to covalently attach the amino-functionalized silica NP to the coated COP surface. The nanoparticle density/distribution was then imaged using AFM (Supporting Informations). Figure 3 shows the NPs amount per micron square on all coatings. As expected, the uncoated Zeonor® surface was unreactive. At fixed deposition time (4 min), the bounded NPs number

was very similar for plasma powered at 7 and 14 watt. Then, it declined with increase of power to 25 watt. At fixed RF power (14 watt), the attached NPs number increased to a maximum value with increasing deposition time. So, coatings presenting the highest amount of free NH_2 (as indicated by PMIRRAS spectroscopy) attached the highest NPs amount. In other words, larger amine content resulted in better NP attachment capacity. Although the nanoparticle distribution cannot directly reveal the amount of amine groups on the surface, it can provide an idea of their density, distribution and their capability to bind nano-objects. However, this nanoparticle approach has some limitations mainly due to surface saturation, which makes the method dependent on NP size, for example. Moreover, the coating stability and presence after different washing steps is confirmed through those experiments as NPs are still observed at the end of the process. Remembering the admitted coating formation process, APTES fragments formed into the plasma chemisorb (i.e., form covalent link) onto the surface upon deposition (which is not the case for EDA fragments on COP). The presence of Si-O- groups apparently plays an important role in the formation of chemisorbed amino coatings onto activated polymeric substrates.

Figure 3

To further investigate the reactivity of preselected coatings (14 watt – 4 min and 7 watt – 4 min), the coupling reaction of aminated surfaces to an amine-reactive fluorophore was studied. Figure 4 shows on the 14 watt – 4 min coating double intensity that on the 7 watt – 4 min coating, indicating the presence of twice the amount of reactive surfacial amino groups, if we assume one fluorophore per surfacial amino group. Although both selected coatings presented similar NP attachment, they behaved significantly differently while attaching

fluorophores. This is probably due to size effects: the nanoparticles used were ~ 60 nm in diameter; the fluorophore has a size in the nanometre range.

Figure 4

To demonstrate biomolecule binding capacity, DNA attachment was performed. Fluorescence intensities measured after attachment of a polynucleotide (Figure 4) indicated the 14 watt coated surface to be three times more performant in attaching DNA molecules than the 7 watt coated one. However, the PMIRRAS NH_2 peak area was twice larger in the 7 watt deposited films than in the 14 watt film. This indicates that, whilst there could have been more amines in the 7 watt coating than in the 14 watt, either they were not present at the surface or they were not reactive. It seems unlikely that the coating varied significantly in its composition through its thickness. We deduced earlier that one effect of increasing the plasma power was to increase fragmentation of the silane. Thus, we speculate that, in the layer formed with 7 watt power, the formation of a layer from largely intact silane also resulted in a network that bonded and constrained the amine groups within the interior of the layer. Fragmentation of the silane could produce ethoxy and alkyl amino radicals. One hypothesis is that insertion of alkyl amino radicals into the network at the surface of the growing film was responsible for creating the higher amount of surface reactive amines present in the film formed with a higher power.

Figure 5

The applicability of such coatings for biosensor platforms was demonstrated through an antibody/antigen bioassay, Figure 5. The 14 watt – 4 min APTES coated slide was employed

in a typical sandwich immunoassay format using gαIgG and Cy5-labeled gαIgG as capture and detection antibodies respectively, and IgG as the model analyte. The limit of detection (corresponding to the background signal plus 3 times the standard deviation of the background signal) was determined to be 5.7 pg ml^{-1}. This value is two orders of magnitude better than the ones obtained with immunosensors modified by silanization in solution (Boozer 2006; Vikholm-Lundin and Albers 2006). Further, such APTES coated COP slides appears to be stable over time as contact angle values are fairly stable even after 5 week while stored in air (unpublished data), increasing the possible future applications of such platform in commercial biosensor and biomedical diagnostics applications.

4. Conclusions

Cycloolefin polymer surfaces were successfully functionalized through the PECVD deposition of a new precursor, APTES, yielding amine functional groups available for biomolecule attachment. The deposition conditions were optimized in order to gain the most performant surface in attaching nanoparticles and DNA molecules. We identified the effect of plasma power in both activating and fragmenting the silane, and in both building the layer and eroding it. The consequences were that, in our system, whilst the thickness of the layer could be increased by increasing power and deposition time, the chemical functionality was optimal at a specific combination of parameters. We speculated that the effect of fragmentation of the silane into siloxane, ethoxy and alkyl amine radicals was the determining factor. An immunoassay performed using human IgG as a model analyte shows an improvement of the detection limit by two orders of magnitude beyond that obtained using devices activated by liquid-phase reaction.

5. Acknowledgements:

This material is based upon works supported by the Science Foundation Ireland (S.F.I.) under Grant No. 05/CE3/B754. D.E.W. is an E.T.S. Walton Visiting Fellow of Science Foundation Ireland. C.V. is a postdoctoral researcher of the Belgian Fund for Scientific Research (F.R.S./F.N.R.S.).

6. References

Arriagada, F.J., Osseo-Asare, K., 1999. J. Colloids Interface Sci. 211, 210-220.

Bae, I.-S., Jung, C.K., Cho, S.-J., Song, Y.-H., Boo, J.H., 2007. J. Korean Phys. Soc. 50, 1854-1857.

Boozer, C., Ladd, J., Chen, S., Jiang, S., 2006. Anal. Chem. 78, 1515-1519.

Cho, Y., Ivanisevic, A., 2004. J. Phys. Chem. B 108, 15223-15228.

Diaz-Quijada, G.A., Peytavi, R., Nantel, A., Roy, E., Bergeron, M.G., Dumoulin, M.M., Veres, T., 2007. Lab Chip 7, 856-862.

Di Mundo, R., Ricci, M., d'Agostino, R., Fracassi, F., Palumbo, F., 2007. Plasma Process Polym. 4, S21-S26.
Dudek, M.M., Gandhiraman, R.P., Volcke, C., Cafolla, A.A., Daniels, S., Killard, A.J., 2009a. Langmuir 25, 11155-11161.
Dudek, M.M., Gandhiraman, R.P., Volcke, C., Daniels, S., Killard, A.J., 2009b. Plasma Process Polym. 6, 620-630.
Dreesen, L., Silien, C., Volcke, C., Sartenaer, Y., Thiry, P.A., Peremans, A., Grugier, J., Marchand-Brynaert, J., Brans, A., Grubisic, S., Joris, B., 2007. ChemPhysChem 8, 1071-1076.
Haïdopoulos, M., Mirabella, F., Horgnies, M., Volcke, C., Thiry, P.A., Rouxhet, P., Pireaux, J.J., 2007. J. Microscopy 228, 227-239.
Gandhiraman, R.P., Daniels, S., Cameron, D.C., 2007. Plasma Process Polym. 4, S369-S373.
Gandhiraman, R.P., Karkari, S.K., Daniels, S., MacCraith, B.D., 2009. Surf. Coat. Tech. 203, 3521-3526.
Jönsson, C., Aronsson, M., Rundström, G., Pettersson, C., Mendel-Hartvig, B., Bakker, J., Martinsson, E., Liedberg, B., MacCraith, B.D., Öhman, O., Melin, J., 2008. Lab chip 8, 1191-1197.
Jung, D., Yeo, S., Kim, J., Kim, B., Jin, B., Ryu, D.-Y., 2006. Surf. Coat. Technol. 200, 2886-2891.
Kanan, S.M., Tze, W.T.Y., Tripp, C.P., 2002.. Langmuir 18, 6623-6627.
Kim, J., Park, H., Jung, D., Kim, S., 2003. Anal. Biochem. 313, 41–45.
Kulisch, W., Lippmann, T., Kassing, R., 1989. Thin Solid Films 174, 57-61.
Kurth, D.G., Bein, T., 1995. Langmuir 11, 3061-3067.
LaGraff, J.R., Chu-LaGraff, Q., 2006. Langmuir 22, 4685-4693.
Mateo-Martí, E., Briones, C., Román, E., Briand, E., Pradier, C.M., Martín-Gago, J.A., 2005. Langmuir 21, 9510-9517.
Muguruma, H., Kase, Y., 2006. Biosens.Bioelectron. 22, 737–743.
Qian, W., Yao, D., Xu, B., Yu, F., Lu, Z., Knoll, W., 1999. Chem. Mater. 11, 1399-1401.
Raj, J., Herzog, G., Manning, M., Volcke, C., McCraith, B.D., Ballantyne, S.,Thompson, M., Arrigan, D.W.M., 2009. Biosen & Bioelectron. 24, 2654-2658.
Simon, A., Cohen-Bouhacina, T., Porté, M.C., Aimé, J.P., Baquey, C., 2002. J. Colloid Interface Sci. 251, 278-283.
Socrates, G., 2004. Infrared and Raman Characteristic Group Frequencies,Wiley VCH, Chichester.
Song, S., Zhou, J., Qu, M., Yang, S., Zhang, J., 2008. Langmuir 24, 105-109.
Vikholm-Lundin, I., Albers, W., 2006. Biosen. & Bioelectron. 21, 1141-1148.
Wavhal, D.S., Zhang, J., Steen, M.L., Fisher, E.R., 2006. Plasma Process Polym. 3, 276-287.
White, L.D., Tripp, C.P., 2000. J. Colloid Interface Sci. 232, 400- 407.
Zhang, F., Srinivasan, M.P., 2004. Langmuir 20, 2309-2314.

7. Figures

Table 1: Table presenting (1) the thickness; (2) the water contact angle and (3) the mean roughness of the PECVD deposited coating.

Figure 1: PMIRRAS spectra of bare COP surfaces (black) and PECVD coating on COP surfaces deposited at fixed deposition time (4 min) and varying RF plasma power of 7 watt (red), 14 watt (green) and 25 watt (blue). Three region of interest are highlighted: 1300-1000 cm^{-1} (region 1), 1800-1500 cm^{-1} (region 2) and 3500-3200 cm^{-1} (region 3).

Figure 2: PMIRRAS spectra of bare COP surfaces (black) and PECVD coating on COP surfaces deposited at fixed RF plasma power (14 watts) and varying deposition time of 2 min (red), 4 min (green) and 8 min (blue). Three region of interest are highlighted: 1300-1000 cm^{-1} (region 1), 1800-1500 cm^{-1} (region 2) and 3500-3200 cm^{-1} (region 3).

Figure 3: Graphical representation of the number of nanoparticles attached per micron square on coated COP surfaces at fixed deposition time (left) and fixed RF plasma power (right).

Figure 4: Fluorescence intensity measured after fluorophore (bottom) and DNA attachment (top) on the 7 watt – 4 min and 14 watt - 4 min coatings.

Figure 5: Fluorescence linked immunosorbent assays for the detection of IgG as the model analyte.

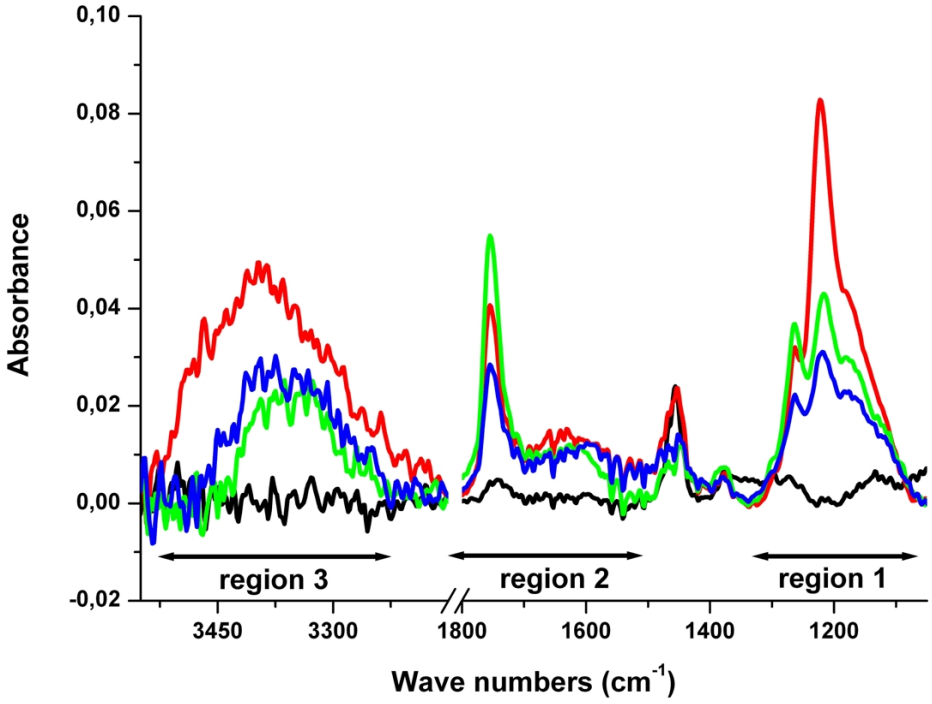

Figure 1

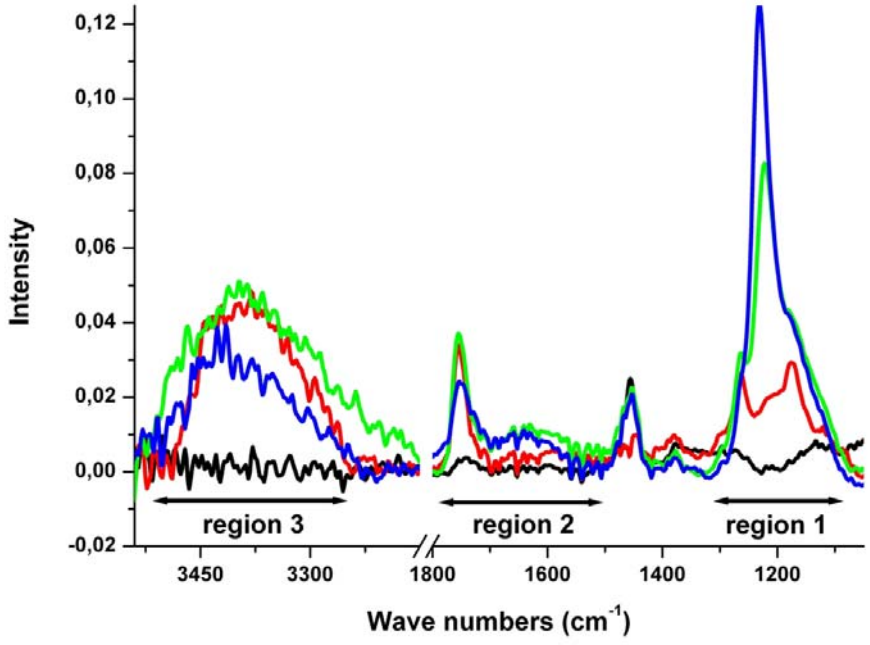

Figure 2

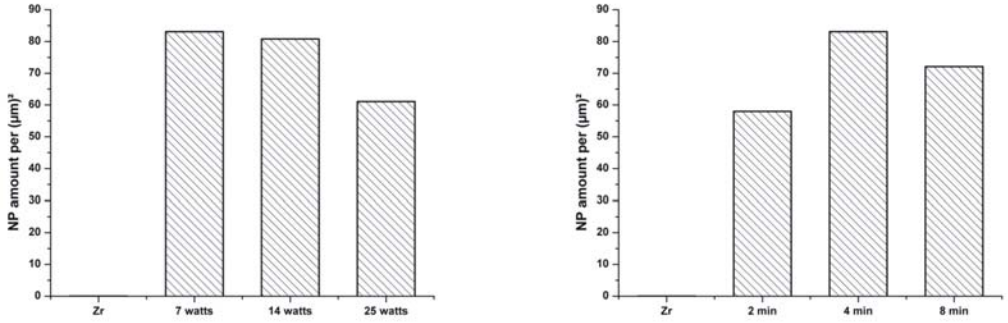

Figure 3

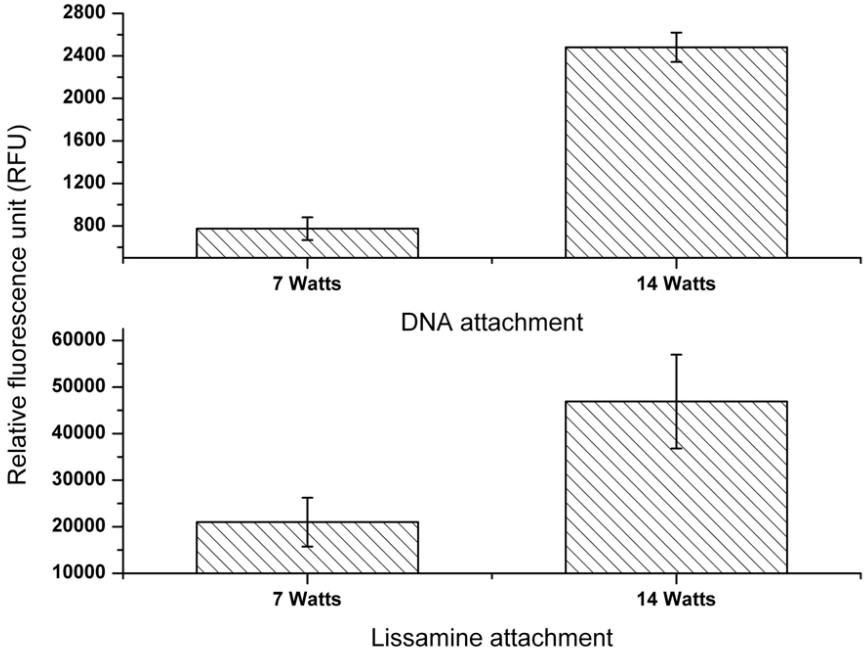

Figure 4

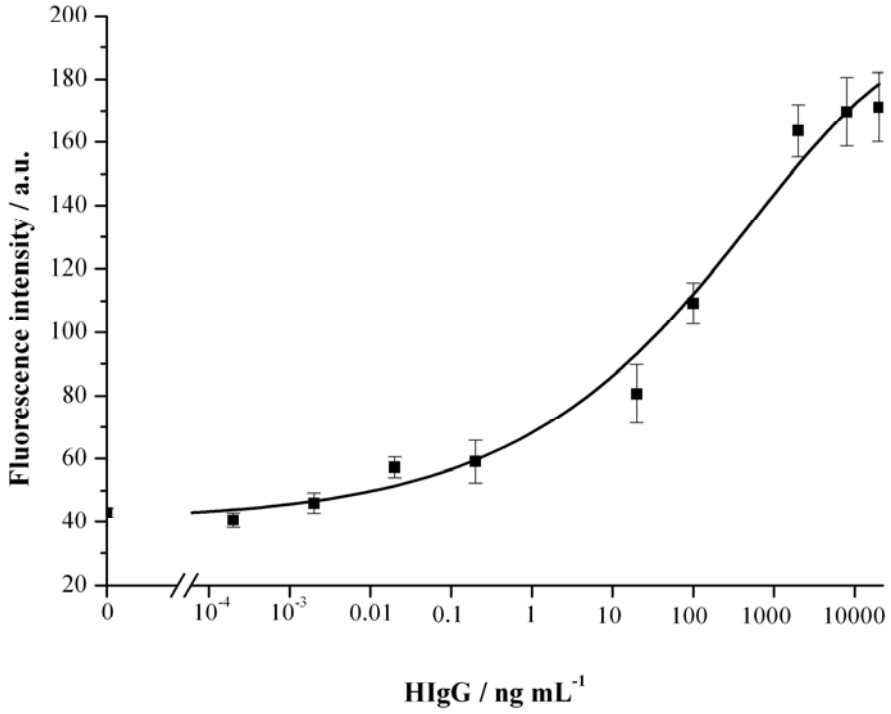
Fluorescence intensity / a.u.
200
180
160
140
120
100
80
60
40
20
0
10-4
10-3
0.01
0.1
1
10
100
1000
10000
HIgG / ng mL-1

Figure 5

Deposition conditions	Layer thickness (nm)	Water contact angle (°)	Surface roughness R_{rms} (nm)
Zeonor®		92.2 ± 2.3	0.5 ± 0.1
4 min 7 watts	9.0 ± 0.1	58.2 ± 1.4	1.4 ± 0.3
4 min 14 watts	13.4 ± 0.3	60.6 ± 2.5	0.7 ± 0.1
4 min 25 watts	19.2 ± 0.3	56.5 ± 1.1	1.2 ± 0.2
14 watts 2 min	3.4 ± 0.1	55.4 ± 1.7	1.3 ± 0.1
14 watts 4 min	13.4 ± 0.3	58.2 ± 1.4	0.7 ± 0.1
14 watts 8 min	17.2 ± 0.3	60.0 ± 1.0	0.9 ± 0.1

Table 1